Title

Three-Dimensional Printing in Combined Cartesian and Curvilinear Coordinates

Authors

Shi, Edward
Lou, Leo
Warburton, Linnea
et al.

Peer reviewed

Technological Brief

3D printing in combined cartesian and curvilinear coordinates

Edward Shi[1, 2]*, Leo Lou[3]*, Linnea Warburton[1,#], Boris Rubinsky[1,3]

1 Department of Mechanical Engineering, University of California Berkeley
2 Department of Mechanical Engineering, University of Colorado, Boulder
3 Department of Bioengineering, University of California Berkeley
*Equal first co-authors
Corresponding author < >

Abstract:

A 3D printing technology that facilitates continuous printing along a combination of cartesian and curvilinear coordinates, designed for *in vivo* and *in situ* bioprinting is introduced. The combined cartesian/curvilinear printing head motion is accomplished by attaching a biomimetic, flexible, "tendon cable" soft robot arm to a conventional cartesian three axis 3D printing carousel. This allows printing along a combination of cartesian and curvilinear coordinates using five independent stepper motors controlled by an Arduino Uno with each motor requiring a microstep driver powered via a 12V power supply. Three of the independent motors control the printing head motion along conventional cartesian coordinates while two of the independent motors control the length of each pair of the four "tendon cables" which in turn controls the radius of curvature and the angle displacement of the soft printer head along two orthogonal planes. This combination imparts motion along six independent degrees of freedom in

cartesian and curvilinear coordinates. The design of the system is described together with experimental results which demonstrate that this design can print continuously along curved and inclined surfaces while avoiding the "staircase" effect, which is typical of conventional three axis 3D printing along curvilinear surfaces.

Introduction

There are numerous emerging applications for 3D printing in medicine and bioengineering. For example, there is growing interest in 3D printing for *in vivo* and *in situ* applications in the body, such as treatment of stomach ulcers, printing of skin substitutes on the body of the patient or under the skin [1], [2], [3], [4]. The use of 3D printing models of parts of the body prior to surgery, has also become common, e.g. [5], [6]. Most 3D printers operate in three cartesian axes, print along the cartesian axis and generate objects with mostly isotropic properties along the cartesian axes. Conventional 3D printing objects are generated by depositing layer on top of layer along the cartesian axes using a planar surface as the basis for the printing. However, tissues in the body are anisotropic, often with different anisotropic material properties along a curvilinear axis.

Attempts to generate anisotropic printing along curvilinear coordinates with conventional three axis degrees of freedom printers results in staircase structures with flaws in mechanical properties because of the cartesian planar mode of deposition [7], [8]. For example in 3D printing of a skull model, the outer surface of the skull has a stair-like appearance and the mechanical properties of the skull are defined by the planes of the printing surface [8]. However, obviously, the skull has smooth outer surface, and the skull properties are anisotropic along the outer surface of the skull. A solution was proposed in reference [8], which entails printing on top of a mandrel. However, using a mandrel requires an additional step in manufacturing.

It should be emphasized that issues with printing on curvilinear or irregular surfaces are not unique to bioengineering. For example, the challenge of printing on surfaces with irregular electronic components [9] or the printing of an airplane wings in which a conventional 3D cartesian printed surface has a step wise appearance [10].

Because of the emerging importance of 3D printing along irregular and curvilinear surfaces, substantial research was recently published in the field. A good review of the issues related to printing along cartesian axis of irregular and curvilinear coordinates surfaces can be found in [11]. These include shape form problems as well as undesirable mechanical properties,

MED-21-1239   Corresponding Author: Warburton

in particular between the 3D printed layers. The main approach to printing along anisotropic and curvilinear coordinates is to increase the number of degrees of freedom of the printer head carousel using multiple degrees of freedom robotic arms. For example, Keating et al developed a six degrees of freedom robotic arm [12], Zhang et al used two nozzles and five degrees of freedom axis [13], Dai et al used five degrees of freedom axis and two rotational degrees of freedom [14], Fry et al used two robotic arms which in combination give multiple degrees of freedom [15], van Kampen et al used four axis [16]. Analyzing these papers, it becomes obvious that all these designs impart additional degrees of freedom to the platform on which a rigid nozzle is attached. Concepts from robotics are used to generate the additional degrees of freedom. The devices that impart these degrees of freedom are located behind the printer nozzle and their function is to bring the rigid nozzle to the site at which the printing ink is deposited. The devices (robot arms) that move the 3D printing platform with the rigid nozzle are large and occupy much space. While cumbersome in general, these 3D printing systems are not suitable to print in small places, such as in the body or in small scale electronics.

This "Technological Brief" describes a technology that can generate multiaxial degrees of freedom with a very small device footprint, that is suitable for 3D printing in surgery and for electronics. The key innovation is the use a flexible soft robotic printing arm for the printing nozzle rather than

a rigid printing nozzle. The device combines conventional three axis 3D printing along cartesian coordinates with a flexible soft robot printing arm that can move unconstrained in the 3D space along combined cartesian and curvilinear coordinates. The system employs a flexible, soft, robotic arm with a biomimetic design inspired by the octopus's arm. The advantage of this technology over conventional multi-axis robots with rigid arms is that it is not confined to the degrees of freedom of the rigid robotic arms, as many as there may be, and its footprint is very small and therefore may be more suitable for printing in confined spaces, such as in vivo and in situ. There are many designs for a flexible robot arm, and some of them are reviewed in [17]. To illustrate the additive manufacturing concept proposed here, in this study we use a variant of a cephalopod robotic arm, also known as a "tendon cable" robot arm [18]. We chose this type of soft robot printing head because mimicking nature tends to produce designs that can do a larger variety of tasks, and thus may have advantages in the future of 3D bioprinting in the body.

Design principle of the flexible robot arm

As mentioned earlier, there are many designs for flexible robot arms and numerous studies on tendon cable type soft robot arms, e.g. [19]. In Figure 1A we illustrate the concept of a tendon cable robot arm through a schematic. The basic element of a tendon cable robot arm is a central

MED-21-1239   Corresponding Author: Warburton

flexible backbone that is rigidly attached to an anchor plate and to vertebrae along the backbone, and to an end vertebra. Other basic elements are tendons, which while rigidly attached to the end vertebrae (plate) can move freely through holes in all the other vertebrae and the anchor plate. The flexible robot arm achieves movement through the tension and relaxation of multiple tendons. As seen in Fig. 1B, robot arm movement is achieved through tightening of the bottom tendon and relaxation of the top tendon. Fig 1B illustrates the motion of the constant length backbone when the bottom tendon is shortened by a length, dx, while the top tendon is allowed to extend. The fixed length of the flexible backbone, L, the distance between the point of connection of the flexible backbone and the fixed point of the tendon, a, on the last vertebrae and the shortening of the bottom tendon, dx, can be used to calculate the angle, $d\theta$ and the radius of rotation, R, of the flexible backbone. The two geometrical equations below give the relation between the curvature that is imparted to the printing head when attached to the flexible backbone and the end vertebrae and shortening the length of the bottom tendon by, dx.

$$(R-a)d\theta = (L-dx)$$ (1)

$$Rd\theta = L$$ (2)

These two equations give the following expressions, from which the curvature path which the printing head will follow can be calculated.

$$d\theta = \frac{dx}{a} \; ; R = \frac{La}{dx}$$

(3)

Large numbers of tendons as well as combinations of several continuous units such as the one in Figure 1A, can generate any complex motion in the 3D space, in a way that mimics the motion of an octopus arm.

Means to generate the motion of the flexible robot arm

The tensioning and relaxation of the tendon wires is caused by a torque on a pulley to which they are attached. The motion of the pulley is generated by a stepper motor. In order to ensure repeatable, reliable arm movement along curvilinear coordinates, the constant length flexible backbone is rigidly attached to the anchor plate, which in turn is rigidly attached to the 3D printer carrousel. All of the vertebrae are also rigidly attached to the flexible backbone, and the pulleys are fixed on the 3D printer carousel. The pretension wire tentacles are attached to the pulley on one end, to the last vertebrae at the other end and pass freely through holes in all the vertebrae (Fig 1A). This allows the flexible arm rotation to be determined by the displacement of the tendons by the pulley. Through tensioning and relaxing

of the opposite tendon wires, the arm can achieve a predetermine, rotational movement along one plane, as given by equation (3).

In our design the flexible robot arm contains two pulleys, each powered by a stepper motor and each driving tendon wires, which are mounted perpendicular to each other. This allows the robot arm to move in a rotational, curvilinear motion along two perpendicular planes, with the winding of the pulley, dx, prescribing the rotation of the flexible robotic printer head in one plane.

As mentioned earlier, the pulley and the rigid anchor plate are rigidly attached to the carousel of the conventional 3D printer. A programmable motion of the printer carousel along the cartesian coordinates, x,y,z, in superposition with the programmable curvilinear motion of the flexible robot arm generated by the pulleys yields a complex motion of the printing head along a combination of cartesian and curvilinear axes.

Design of the flexible robot arm

Figure 2A is a photograph of the assembled device. The device is designed around a conventional 3D printer (FlashForge, Creator Model, LA, CA, USA). The flexible robot arm is connected to the original carriage of the 3D printer, which serves as the rigid base plate for the assembly and provides for

MED-21-1239   Corresponding Author: Warburton

motion along the x, y, z, cartesian coordinates. The carriage in the original 3D printer moves in the x, y plane, while the printing bed provides the motion along the z, axis. Two 42BYGHB stepper motors (Changzhou Bo Hong Electric Appliance Co.,Ltd) are rigidly attached to the FlashForge printer carriage. One of these motors controls the X- plane rotation of the flexible robotic arm and the other controls the Y-plane rotation of the flexible robot arm through pulley belts to which the tendons are attached in orthogonal pairs. The flexible robot arm rotation in the x and y planes is uniquely correlated to the motion of the tendons, as illustrated in Figure 1B and results in a motion along a predictable radius of curvature and angle of rotation. Figure 2B is a higher magnification detail of the rotational motion motors, the pulleys that connect to the tendons and the rigid structure that connects the two motors to the original 3D printer carriage. The design of the rotational motors complex is described in greater details in Figure 4. The printer head consists of a 10mm diameter tube connected to an 18-gauge nozzle that is rigidly attached to the end plate of the flexible robot arm, as shown in Figure 2C. A Harvard PHD 2000 Syringe pump is used to extrude the bioink from a syringe through the 10mm tube for printing (Hollington, MA, US). The cartesian motion motors are the original 3D FlashForge printer motors and provide displacements along the x, y, z coordinates.

Details on the flexible robot arm are shown in Figure 3. Figure 3A shows the entire soft robot arm and the connection to the original 3D printing carousel.

MED-21-1239   Corresponding Author: Warburton

The central flexible backbone is a "UXcell" 1/8"(3mm) Flexible Shaft. The four tendons in this design are made of 1/16" OD insulated electrical wires. They pass through the laser cut vertebrae through holes in the four axial directions. The end plate is similar to the vertebrae, but the tendons are rigidly connected to the end plate. The central backbone is passed through the vertebrae and rigidly connected with flanges to each of the vertebrae and to the original 3D printer carousel. Figure 3B is a photograph of outer edge of the soft robotic arm showing the last vertebrae to which the flexible backbone and the tendons are rigidly attached. The figure also shows the vertebrae and the holes through which the tendons can pass.

Figure 4 shows a photograph of the of the rotational motors complex part that generates the motion along the curvilinear coordinates. It shows two rotational stepper motors that are rigidly attached to the original 3D printing carousel. Pulleys attached to the rotational motion translate the rotational motion of the motors to the displacements of the orthogonal pairs of tendons. As illustrated in Figure 1B, the displacement of the tendons, in turn imparts a curvilinear motion of the flexible robot arm as given by equations 1 to 3.

The motion of the printing head is a superposition of motion in cartesian coordinates and in curvilinear coordinates. The stepper motors are all

Corresponding Author: Warburton

controlled by an Arduino Uno with each motor requiring a microstep driver and are powered via a 12V power supply.

The motion of the printer head is controlled through Arduino software that controls five motors, the three original 3D printer motors that impart motion along Cartesian axis and the two stepper motors which impart motion along the curvilinear axis. The Arduino Stepper Library Step function is used to precisely drive the stepper motors. This function takes an integer parameter which represents how many steps a stepper motor moves. These inputs are recorded in local variables, effectively storing the positions of each stepper motor. The step commands are repeated in a loop until certain conditional statements are met. Arduino is used as the device MCU with the 5 stepper motors, and we developed a library based on the Arduino stepper library and the mathematical model for the flexible arm. A function which can predict the printing head position in space and the direction of motion (Base from xyz + flexible arm) is written, and with this information, the printing route is designed.

Results and Discussion

Experiments illustrating the performance of the combination curvilinear and cartesian 3D printer, used a solution of 4% sodium alginate as the bioprinting ink. Sodium alginate is a widely used naturally occurring biomaterial, preferred for its biocompatibility, easily tunable properties, and

biodegradability. As a result of its numerous favorable properties and similarity to the tissue extracellular matrix, it is frequently used in tissue engineering and for 3D bioprinting [20,21].

The sodium alginate mixture was prepared by adding 4% w/v sodium alginate powder (molecular weight: 222g/mol) (Spectrum Chemical Mfg. Corp. Gardena, CA) to deionized (DI) water. The solution was then mixed on a magnetic stir plate until homogenous and then allowed to settle in the refrigerator (set to 4°C) for at least 24 hours before use. For crosslinking, a 2% w/v solution of calcium chloride ($CaCl_2$) was made by adding 4g of $CaCl_2$ dihydrate powder (Fisher Scientific, Fairlawn, NJ) to 200ml of water. The $CaCl_2$ solution was placed in an atomizer spray bottle and sprayed on the printed structure after printing was complete to induce cross linking.

Figures 5A and 5B, illustrate the printing of curvilinear shapes on a flat surface tilted at an 80° angle to the original 3D printing cartesian axes. In this setup, 4% sodium alginate was printed onto a maximum curve of x^2+2x with an accuracy of up to ±1 mm.

Figures 6A and 6B, illustrate the printing of curvilinear shapes on a curved inclined surface with an angle of 18°. The additional material attachment shows a video of the printing process in Figure 8. It is particularly interesting to notice the continuous print along curved and tilted surfaces.

Conventional 3D printing generates an object by printing flat layers on flat layers, on printing planes defined by the cartesian coordinates of the printer. This is bound to generate steps in the printed object at the resolution of the printer. Printing a continuous line along the inclined and curvilinear surfaces of Figs 5 and 6 cannot be achieved with conventional 3D printers. Figure 7 illustrates how printing along curved surface will appear when made with a 3D cartesian printer and with this combination curvilinear printer. Figure 7A, illustrates that with the curvilinear printer the material is deposited along the radius of curvature. It generates a smooth surface. Figure 7B illustrates the step like structure which is generated along the curved surface. In addition to the fact that the outer surface is not smooth, there will be a mechanical problem when stresses are exerted along the curvilinear surface. It has been established that the material can withstand stresses along the continuous printed surface layers. However, the strength of the material between layers is much less and they tend to delaminated [11]. 3D cartesian coordinates printers are much less expensive that the multi axis printers, and therefore, if there is no concern of anisotropic stresses and smoothness of surface, they are advantageous over multi-axis printers. However, when a design requires the printed object to withstand anisotropic stresses or smooth surfaces along curvilinear coordinates, multi axis printers must be used.

The design in this Technical Brief is part of the family of multiaxial printers. Relative to other multiaxial printers this design is less bulky and requires fewer motors than its other multi axis counterparts. Other multi-axis robot arms are often bulky and have a motor for each degree of freedom. Our design saves on material and motors (power and cost). In terms of effectiveness and economy, the design uses the well-established technology of stepper motors which are already used commonly in 3d printers. There are drawbacks relative to other multiaxial printers. The printing arm is less rigid due to the use of a tendon and flexible backbone rather than pieces of metal attached to other pieces of metal via stiff fasteners. More complex control is required such as software to track the tip of the printer head and plan out the path of the printed part. The technology developed in this Technical Brief is more suitable for use in small spaces such as inside the body or with small scale electronics.

Conclusion:

The combined curvilinear/cartesian printing system of this Technological Brief has the ability to continuously print along any coordinate system cartesian and curvilinear, and thereby print on surfaces whose plane is different from that of the cartesian coordinates of the printer or surfaces that are curved. The capability of the technology described in this paper is particularly relevant to 3D printing in a living organism [3], such as treating wounds [4].It should be mentioned that there are other technologies which

14

are being developed for in vivo and in situ 3D bioprinting. For example using soft robot ferromagnetic printing heads with magnetic actuation [22] or digital near-infrared photopolymerization [23]. These technologies employ complex and expensive devices. In contrast, the technology that we introduce here employs much simpler, mechanical engineering design principles that lend themselves to easy implementation in every engineering laboratory.

List of Figures:

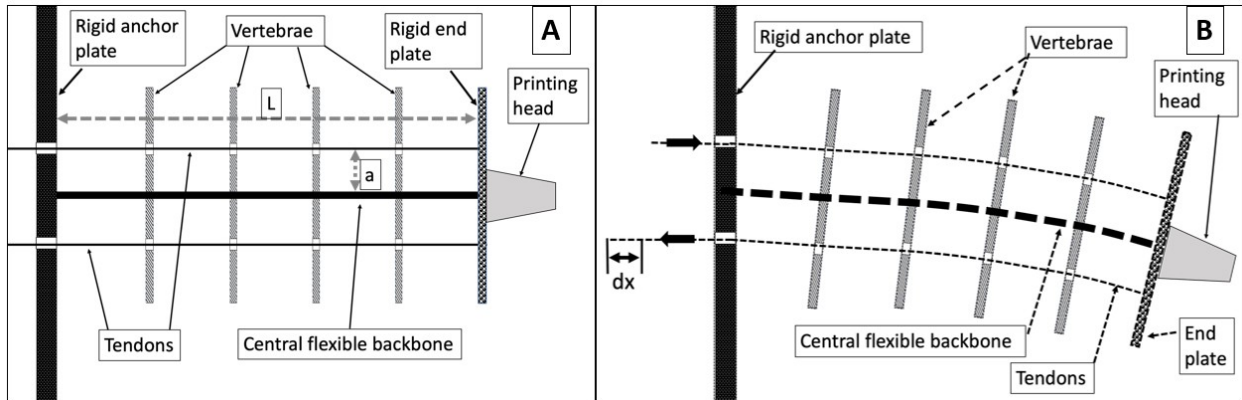MED-21-1239   Corresponding Author: Warburton

Figure 1: Schematic of the flexible robot head printer. A) Design showing the components of the flexible arm. B) Design illustrating how the flexible arm bends.
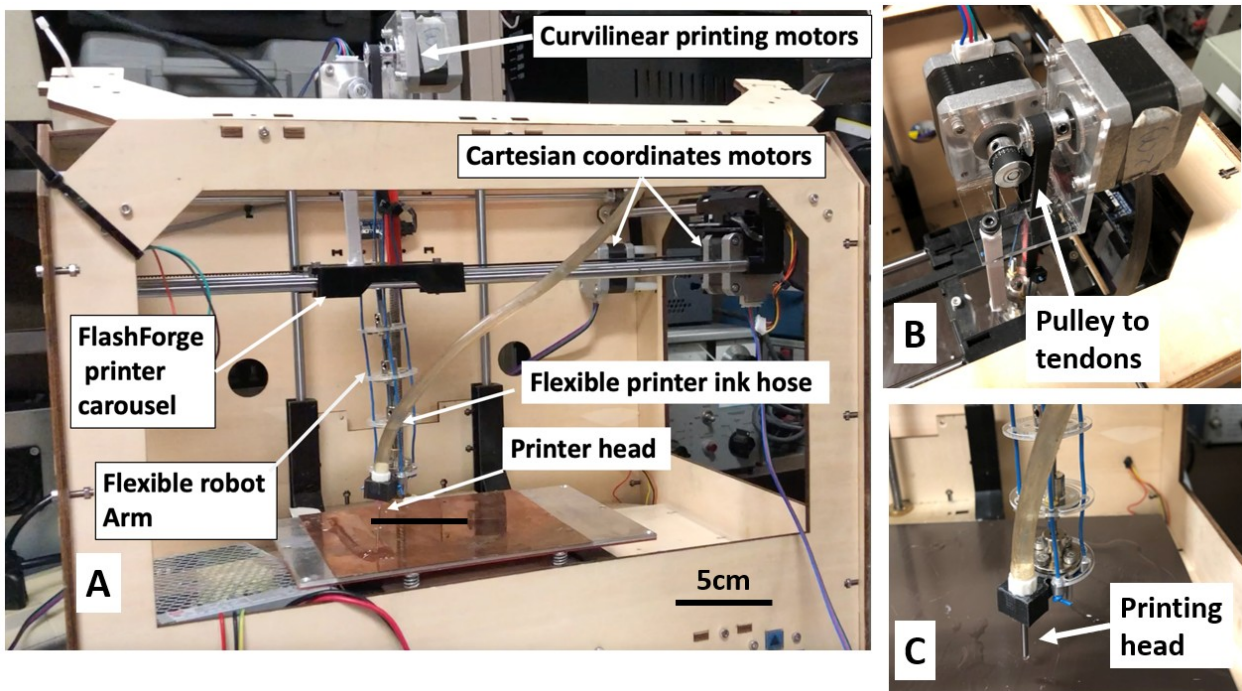
Figure 2: A) An ensemble photograph of the 3D cartesian/curvilinear printer. B) Higher magnification showing the two stepper motors, each of which activates one pair of orthogonal tendons. C) Higher magnification showing the printer head nozzle.
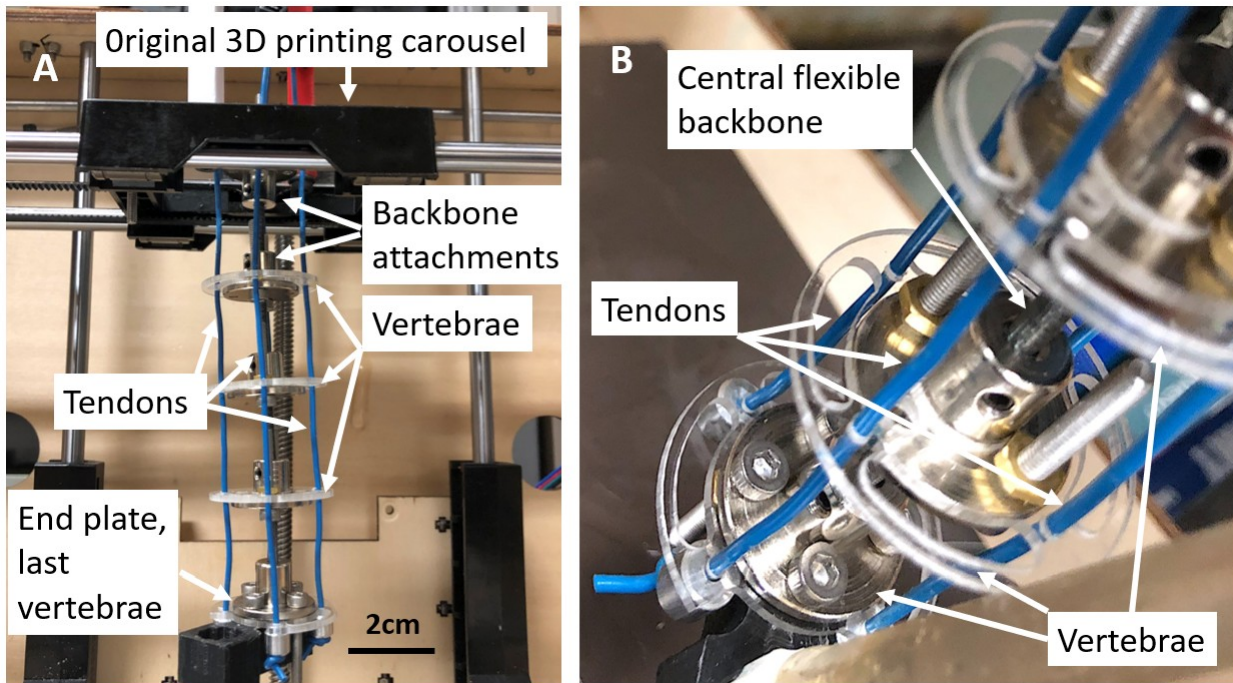
Figure 3: Photographs of the flexible printer arm. A) The complete assembly of the arm with the printer carousel. B) Higher magnifications of the central backbone, tendons, and vertebrae.

Figure 4: View of the 3D printer from the top showing the stepper motors.

Figure 5: Example of printing along an inclined surface. A) The inclined surface at an angle of 80° to the horizontal. B) Printing along the inclined surface at an angle of 80° relative to the horizontal.

Figure 6: Example of printing along a curved surface, with an angle of 18°. A) The printing head, B) Printing along the curved surface with an angle of 18°.

Figure 7: Schematic showing the deposition of the 3D printing ink in A) A curvilinear printer, B) A cartesian coordinates printer. Note the step like surface formed.

Attachment video – please attach this as a video and not a photo.

Figure 1: Schematic of the flexible robot head printer. A) Design showing the components of the flexible arm. B) Design illustrating how the flexible arm bends.

Figure 2: A) An ensemble photograph of the 3D cartesian/curvilinear printer. B) Higher magnification showing the two stepper motors, each of which

activates one pair of orthogonal tendons. C) Higher magnification showing the printer head nozzle.

Figure 3: Photographs of the flexible printer arm. A) The complete assembly of the arm with the printer carousel. B) Higher magnifications of the central backbone, tendons, and vertebrae.
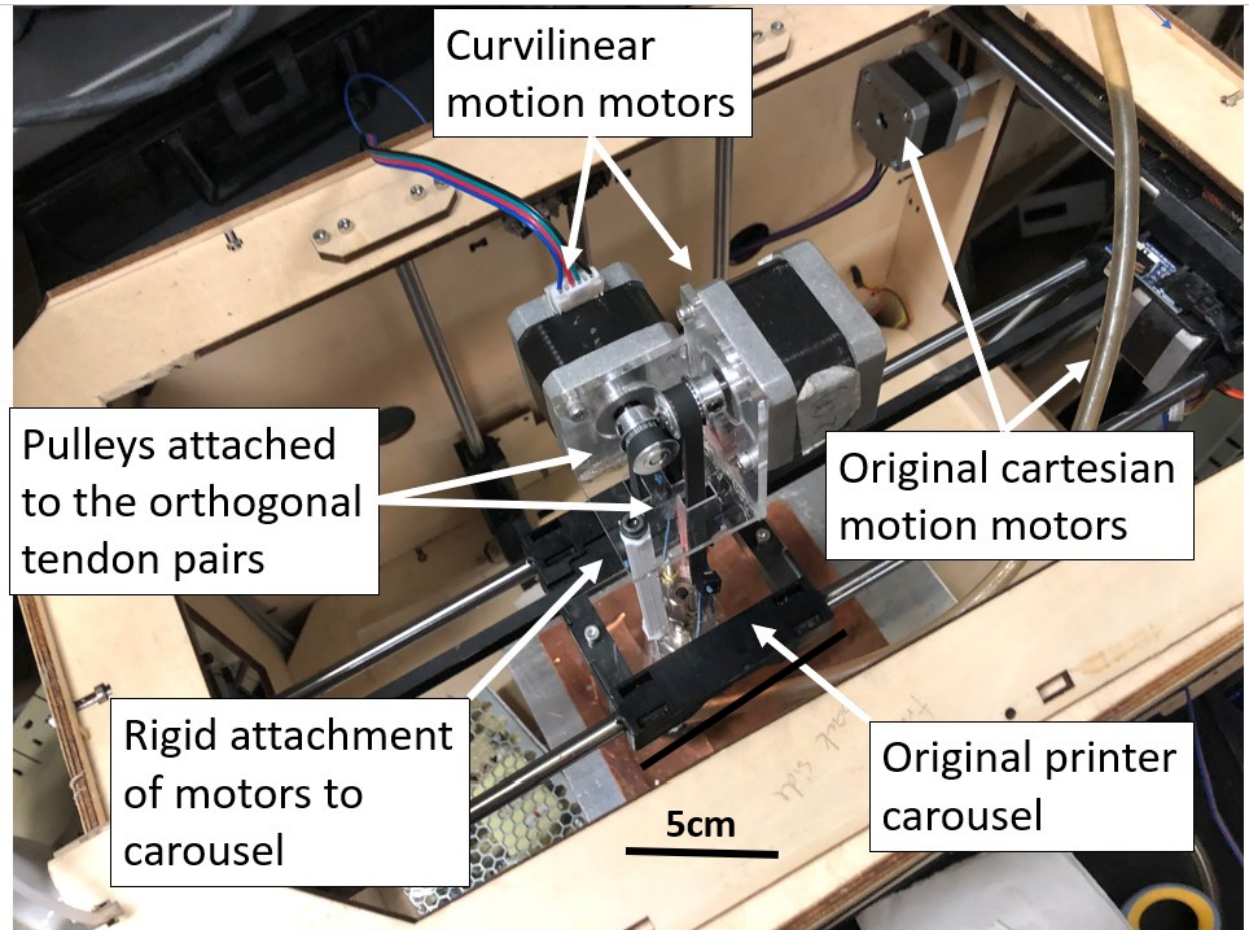
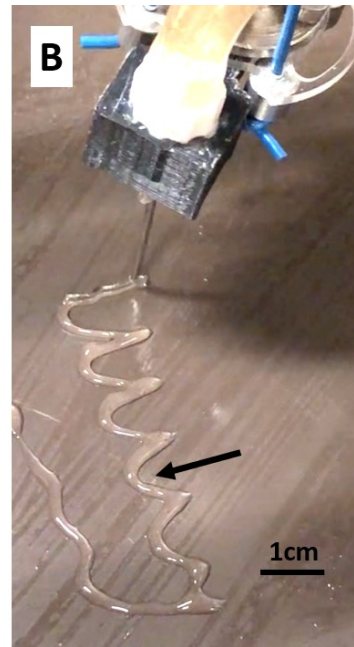Figure 4: View of the 3D printer from the top showing the stepper motors.

Figure 5: Example of printing along an inclined surface. A) The inclined surface at an angle of 80° to the horizontal. B) Printing along the inclined surface at an angle of 80° relative to the horizontal.
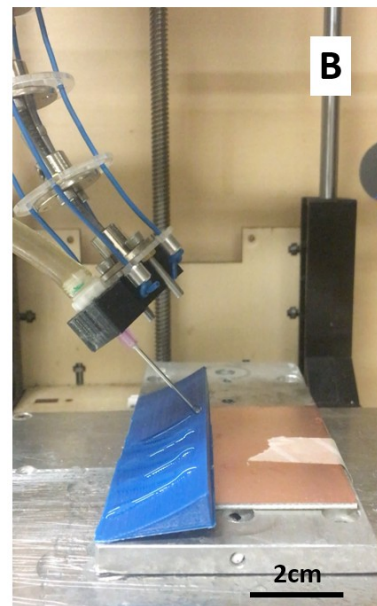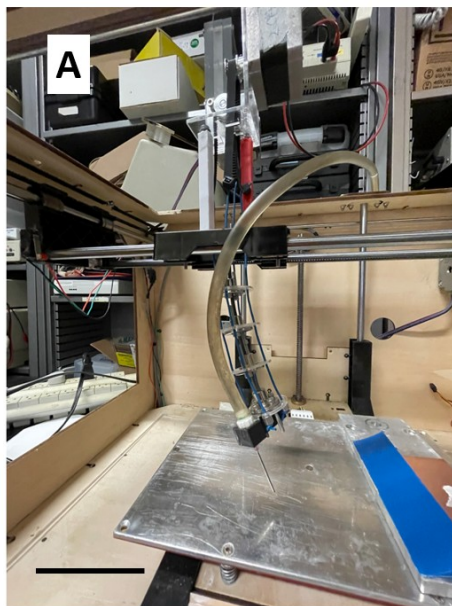
Figure 6: Example of printing along a curved surface, with an angle of 18°. A) The printing head, B) Printing along the curved surface with an angle of 18°.

A) Printing in cylindrical; coordinates along a curved surface

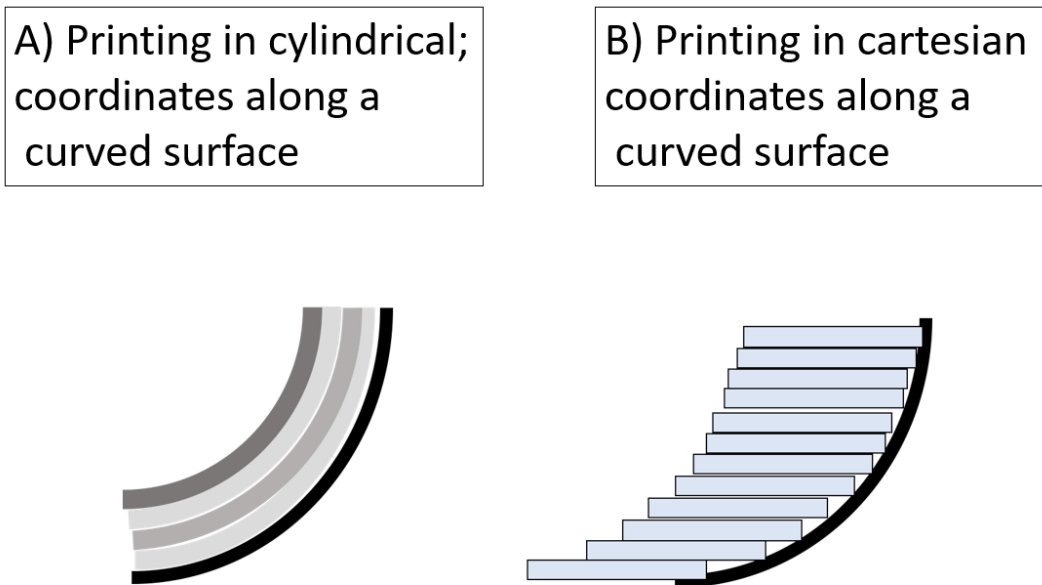B) Printing in cartesian coordinates along a curved surface

Figure 7: Schematic showing the deposition of the 3D printing ink in A) A curvilinear printer, B) A cartesian coordinates printer. Note the step like surface formed.

[1] Keriquel, V., Guillemont, F., Arnault, I., Guillotin, B., Miraux, S., Amedee, J., Fricain, J.-C., and Catros, S., 2010, "In Vivo Bioprinting for Computer- and Robotic-Assisted Medical Intervention: Preliminary Study in Mice," Biofabrication, 2(1), p. 2 014101.

[2] Xhao, W., and Xu, T., 2020, "Preliminary Engineering for in Situ in Vivo Bioprinting: A Novel Micro Bioprinting Platform for in Situ in Vivo Bioprinting at a Gastric Woulnd," Biofabrication, 12(045020).

[3] Urciuolo, A., Poli, I., Brandolino, L., Raffa, P., Scattolini, V., Laterza, C., Giobbe, G.G., Zambaiti, E., Selmin, G., Magnussen, M. and Brigo, L., 2020, "Intravital Three-Dimensional Bioprinting," Nat. Biomed. Eng., 4, pp. 901–915.

[4] Albanna, M., Binder, K.W., Murphy, S.V., Kim, J., Qasem, S.A., Zhao, W., Tan, J., El-Amin, I.B., Dice, D.D., Marco, J. and Green, J. 2019, "In Situ Bioprinting of Autologous Skin Cells Accelerates Wound Healing of Extensive Excisional Full-Thickness Wounds," Sci Rep., 9:1856, p. doi: 10.1038/s41598-018-38366-w.

[5] Ghai, S; Sharma, Y; Pillai, AK; Ghai, Suhani; Sharma, Yogesh; Jain, Neha; Satpathy, Mrinal; Pillai, A. K., 2018, "Use of 3D Printing Technology in Cranimaxxofacial Surgery: A Review," Oral Maxillofac. surgery., 22(3), pp. 249–259.

[6] Erika; Mauri, Valeria; Peri, Andrea; Pugliese, Luigi; Marone, Enrico Maria; Auricchio, F., 2020, "An Overview on 3D Printing for Abdominal Surgery," Surg. Endosc. ultrasound Interv. Tech., 34(1), pp. 1–13.

[7] Tyberg, J., and Bohn, J., 1998, "Local Adaptive Slicing," Rapid Prototyp. J., 4(3), pp. 118–127.

[8] Chakraborty, D., Reddy, B.A. and Choudhury, A.R., 2008, "Extruder Path Generation for Curved Fused Deposition Modeling," Comput. Aided Des., 40(2), pp. 235–243.

[9] Rao, CH; Avinash, K; Goel, S; Rao, C Hanumanth; Avinash, Kothuru; Varaprasad, B K S V L; Goel, S., 2022, "A Review on Printed Electronics with Digital 3D Printing: Fabrication Techniques, Materials, Challenges and Future Oportunities.," J. Electron. Mater., p. DOI: 10.1007/s11664-022-09579-7.

[10] Arigela, S., and Chintamredy, W., 2021, "Fused Deposition Modeling of an Aircraft Wing Using Industrial Robot with Non-Linear Tool Path Generation.," Int. J. Eng., 34(1), pp. 272–282.

[11] Yao, Y., Zhang, Y., Aburaia, M., and Lackner, M., 2021, "3D Printing of Objects with Continuous Spatial Paths by a Multi-Axis Robotic FFF.," Appl.Sci., 11, p. 4825.

[12] Keating, S., and Oxman, N., 2013, "Compound Fabrication: A Multifunctional Robotic Platform for Digital Design and Fabrication," Roabotics Comput. Manuf., 29(6), pp. 439–448.

[13] Zhang H, Lei X, Hu Q, Wu S, Aburaia M, Gonzalez-Gutierrez J, L. H., 2022, "Hybrid Printing Method of Polymer and Continuous Fiber-Reinforced Thermoplastic Composites (CFRTPCs) for Pipes through Double-Nozzle Five-Axis Printer," Polymers (Basel)., 14, p. 819.

[14] Dai, C., Wang, C. C. L., Wu, C., Lefebvre, S., Fang, G., and Liu, Y.-J., 2018, "Support Free Printing by Multi-Axis Motion," C. Trans. Graph., 37(4), pp. 1–14.

[15] Fry, N., Richardson, R., and Boyle, J., 2020, "Robotic Additive Manufacturing System for Dynamic Build Orientations," Rapid Prototyp. J., 26(4), pp. 659–667.

[16] van Kampen, K. A., Olaret, E., Stancu, I. C., Moroni, L., and Mota, C., 2021, "Controllable Four Axis Extrusion-Based Additive Manufacturing System for the Fabrication of Tubular Scaffolds with Tailorable Mechanical Properties," Mater. Sci. Eng. C, 119.

[17] Zhong, Y., Hu, L., and Xu Yinsheng, 2020, "Recent Advances in Design and Actuation of Continuum Robots for Medical Applications," Actuators, 9(14), pp. 142; https://doi.org/10.3390/act9040142.

[18] Walker, I.D., Dawson, D.M., Flash, T., Grasso, F.W., Hanlon, R.T., Hochner, B., Kier, W.M., Pagano, C.C., Rahn, C.D. and Zhang, Q.M., 2005, "Continuum Robot Arms Inspired by Cephalopods," Proc. Soc. PHOTO-OPTICAL Instrum. Eng., 2005(Unmanned Ground Vehicle Technology VII), pp. 303–314.

[19] Renda, F; Giorelli, M; Laschi, C; Renda, Federico; Giorelli, Michele; Calisti, Marcello; Cianchetti, Matteo; Laschi, C., 2014, "Dynamic Modeling of a Multibending Soft Robot Arm Driven by Cables," IEEE Trans. Robot., 30(5), pp. 1109–1122.

[20] Murphy, S. V, Skardal, A., and Atala, A., 2013, "Evaluation of Hydrogels for Bio-Printing Applications," J. Biomed. Mater. Res. Part A, 101(1), pp. 272–284.

[21] Skardal, A., and Atala, A., 2015, "Biomaterials for Integration with 3-D Bioprinting," Ann. Biomed. Eng., 43(3), pp. 730–746.

[22] Zhou, C., Yang, Y., Wang, J., Wu, Q., Gu, Z., Zhou, Y., Liu, X., Yang, Y., Tang, H., Ling, Q. and Wang, L., 2021, "Ferromagnetic Soft Catheter Robots for Minimally Invasive Bioprinting," Nat. Commun., p. 12:5072.

[23] Chen, Y., Zhang, J., Liu, X., and Al, E., 2020, "Noninvasive in Vivo 3D Printing," Sci. Adv., 6(23), p. DOI: 10.1126/sciadv.aba7406.